

Supplementary Material

## Optimizing the Morphology of Calcium D-pantothenate by Controlling Phase Transformation Processes

Dandan Han,<sup>†,‡</sup> Shichao Du,<sup>†,‡</sup> Songgu Wu,<sup>†,‡</sup> Ruiling Ouyang,<sup>†,‡</sup> Junbo Gong<sup>†,‡,\*</sup>

<sup>†</sup> School of Chemical Engineering and Technology, State Key Laboratory of Chemical Engineering,  
Tianjin University, Tianjin 300072, China

<sup>‡</sup> Key Laboratory Modern Drug Delivery and High Efficiency in Tianjin, P. R. China

### **Corresponding author**

\*Tel.: 86-22-27405754. Fax: 86-22-27314971. E-mail: junbo\_gong@tju.edu.cn.

### **1. Solubility measurement process**

The detailed information about the solubility determination of D-PC·4MeOH·H<sub>2</sub>O and D-PC·MeOH are as follows.

To assess thermodynamic stability of these two solvates and obtain the pure crystalline D-PC·4MeOH·H<sub>2</sub>O crystals, the solubility of D-PC·4MeOH·H<sub>2</sub>O and D-PC·MeOH in the binary water + methanol (with the mass content of water as 2%, 5% and 15%) solutions at the temperature of 273.15 K-303.15 K was determined. Before determination, these two solvates were added in water + methanol mixtures with different water content to suspend for about 48 h at the measured temperature, the final solid suspension was used for PXRD determination to identify which solvate is

more stable at the measured conditions. Then, the solubility of the stable solvate was determined by HPLC method. On the other hand, the laser monitoring observation technique was adopted for the unstable solvate solubility determination.

For the stable solvate solubility determination, about 30 mL solvent was put into a 50 mL conical flask, the solution temperature was kept by a thermostatic shaker (type 510A, Shanghai Laboratory Instrument Works Co., Ltd., with an uncertainty of  $\pm 0.1$  K). Then, excess D-PC solvate was added in the solution and stirred for about 12 h to reach the (solid + liquid) equilibrium. After that, the agitation was stopped and the solution was kept still for 2 h to make sure that the undissolved particles settled down. Finally, about 1~5 g supernatant was taken out by the syringe equipped with a 0.22  $\mu\text{m}$  filter. The supernatant was diluted and analyzed by HPLC, each point was repeated three times and the average value was regarded as the final result. While for the unstable solvate solubility determination, 50 g of solvent was added into a 100 mL jacketed vessel with the fixed temperature controlled by temperature controller (Type, CF41, Julabo Technology Co., Ltd), the vessel was sealed with a plug to prevent the solvent evaporation. Then, a fixed amount of D-PC solvate was added into the vessel with a certain interval. At first, the laser beam was blocked by the particles in the solution, so the intensity of laser beam through the vessel was low. The intensity increases gradually with the dissolution of the solute. When D-PC solvate just disappeared, the intensity reached the maximum. Then the additional solute of known mass (0.1~0.3 mg) was added into the vessel, along with which the intensity of the laser decreased immediately. The intensity of laser increased gradually along with the dissolution of the particles and reached the former constant.

This process was also repeated until the solid could not dissolve and the laser intensity kept constant, the system was considered as reaching the phase equilibrium, and the total consumption of the solute was recorded. Each measuring point was repeated three times to obtain the average value as the final result.

## 2. The PXRD pattern and TGA curve of the raw material

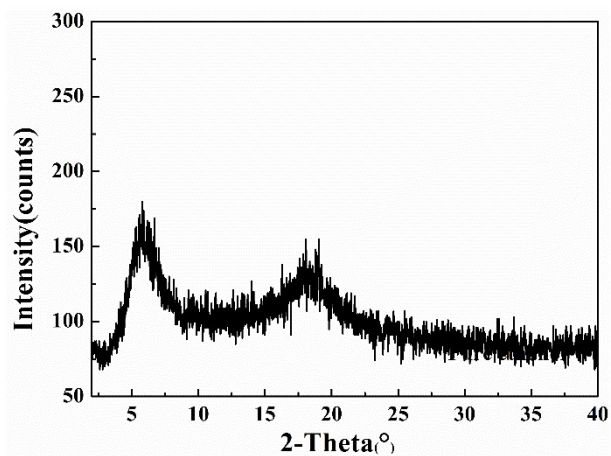


**Figure S1.** The PXRD pattern of the raw material.

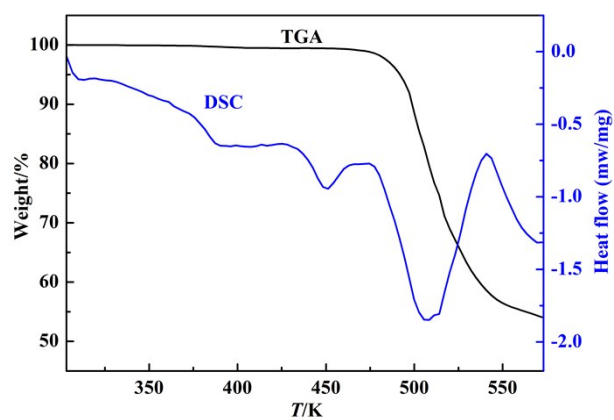


**Figure S2.** The TGA curve of the raw material.

### 3. ATR-FTIR calibration curve

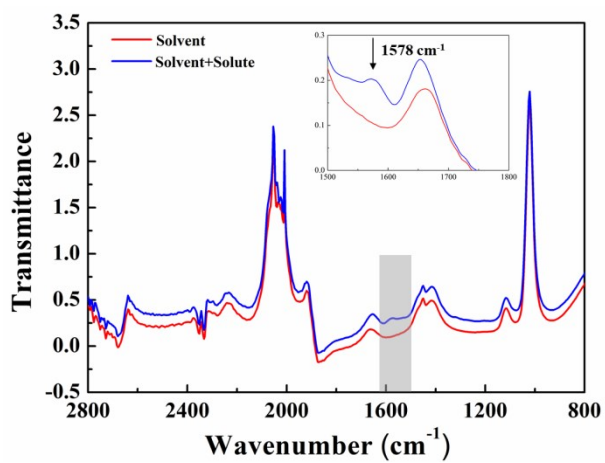


**Figure S3.** ATR-FTIR spectra of the solvent and D-PC in the solution, the peak intensity at  $1578 \text{ cm}^{-1}$  was selected as the characteristic peak to monitor D-PC concentration in real time.

#### 4. ATR-FTIR spectrometry calibration curve

The peak intensity versus concentration (g/100g solvent) calibration curve of D-PC was determined by the ATR-FTIR spectrometry, illustrated in Figure S4. The results illustrate that the calibration curve is linear with  $R^2=0.9994$ , indicating the good correlation between the concentration and peak intensity in the determined concentration range.

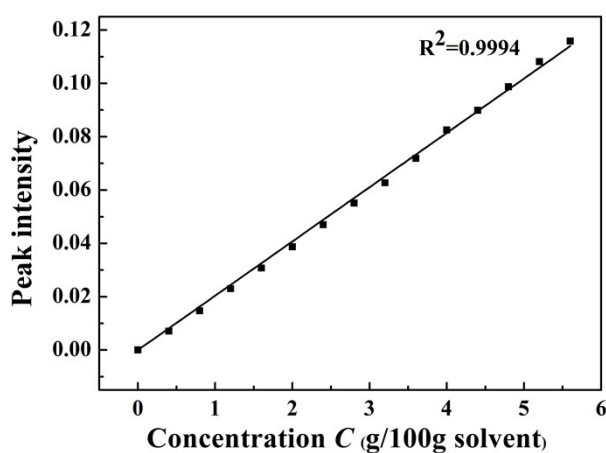


**Figure S4.** Calibration curve of the peak intensity at  $1578\text{ cm}^{-1}$  in ATR-FTIR spectrum versus the concentration of D-PC (100g/g).

## 5. Raman spectra of D-PC·4MeOH·H<sub>2</sub>O and D-PC·MeOH in the solution

In fact, the Raman spectra of these two solvates are actually very similar, because both of these two solvates contain methanol molecules in the crystals. However, by carefully comparing and analyzing the characteristic peaks of the two crystal solvates, we found the Raman shift at 899 cm<sup>-1</sup> and 750 cm<sup>-1</sup> was the best peak to present D-PC·4MeOH·H<sub>2</sub>O and D-PC·MeOH, respectively (Figure S5).

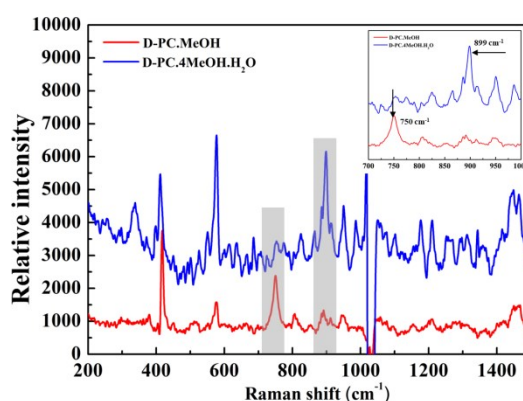


**Figure S5.** Raman spectra of D-PC·4MeOH·H<sub>2</sub>O and D-PC·MeOH in methanol + water mixtures, Raman shift at 899 cm<sup>-1</sup> and 750 cm<sup>-1</sup> was selected to represent D-PC·4MeOH·H<sub>2</sub>O and D-PC·MeOH, respectively.

Moreover, the changes of the Raman spectra of the suspended solid in the solution during crystal phase transformation process are shown in Figure S6. It can be seen that the peak intensity at 750 cm<sup>-1</sup> decreased with time, while the peak intensity at 899 cm<sup>-1</sup> increased with time. This is due to the dissolution of D-PC·MeOH and the growth of D-PC·4MeOH·H<sub>2</sub>O.

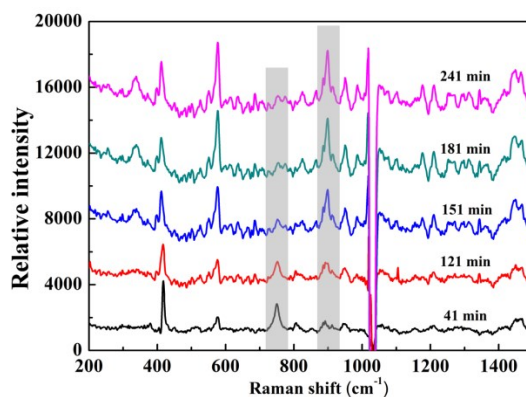


**Figure S6.** D-PC Raman spectra of the suspended solid in the solution during crystal phase transformation process from D-PC·MeOH and D-PC·4MeOH·H<sub>2</sub>O.

Besides, the change in the peak intensity at 750 cm<sup>-1</sup> and 899 cm<sup>-1</sup> with the mass of solid suspension of D-PC·MeOH and D-PC·4MeOH·H<sub>2</sub>O was determined, respectively. It can be seen from Figure S7a that the peak intensity at 750 cm<sup>-1</sup> increased with the increase of solid suspension of D-PC·MeOH, while the peak intensity at 899 cm<sup>-1</sup> shows a very slight increase. Instead, in Figure S7b, the peak intensity at 899 cm<sup>-1</sup> increased with the increase of solid suspension of D-PC·4MeOH·H<sub>2</sub>O, while the peak at 750 cm<sup>-1</sup> showed a very slight increase. Thus, we think that the decreased relative intensity at 750 cm<sup>-1</sup> can be used to represent the decrease of D-PC·MeOH crystals in general, while the increased relative intensity at 899 cm<sup>-1</sup> can be regarded as the increase of D-PC·4MeOH·H<sub>2</sub>O crystals. It should be noted that the relative intensity of the characteristic peak was only used to show the trend of solid-phase composition in the solution during the phase transformation process from D-PC·MeOH to D-PC·4MeOH·H<sub>2</sub>O, rather than giving the precise fraction of these two solvates.

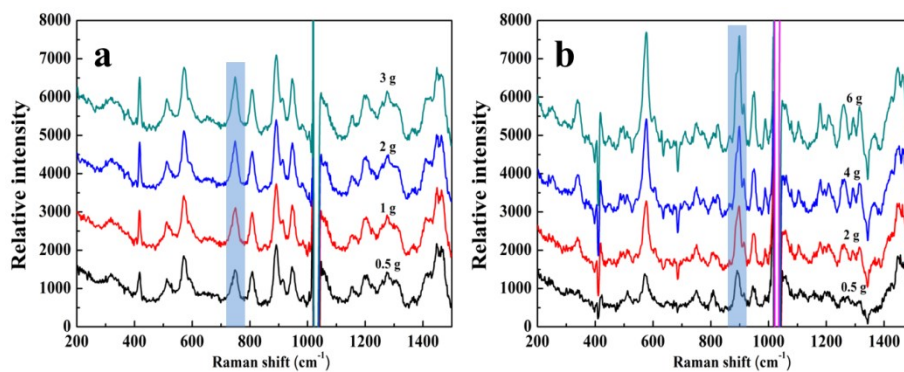


Figure S7. (a) The change in the peak intensity at  $750 \text{ cm}^{-1}$  with the mass of suspension solid of D-PC-MeOH in Raman spectra; (b) The change in the peak intensity at  $899 \text{ cm}^{-1}$  with the mass of suspension solid of D-PC-4MeOH·H<sub>2</sub>O in Raman spectra.

## 6. The PXRD patterns of the residual solids after the solubility

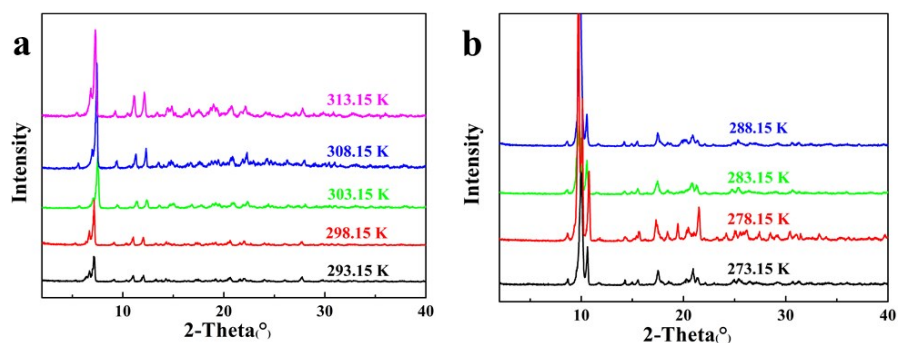


Figure S8. The PXRD pattern of the residual solids after the solubility in water + methanol mixtures with water contents of 2%.

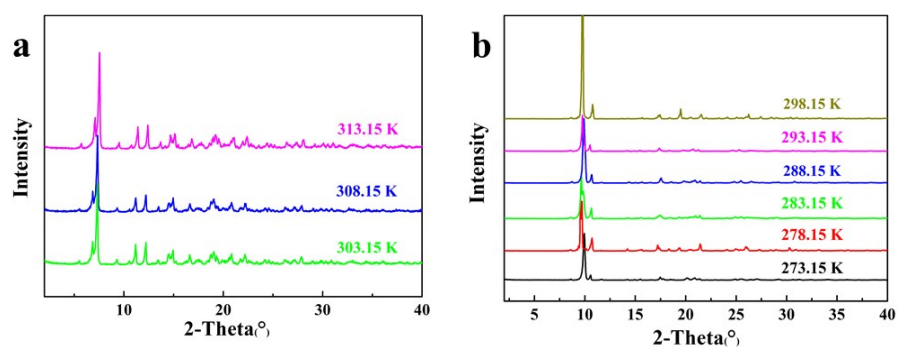


Figure S9. The PXRD pattern of the residual solids after the solubility in water + methanol mixtures with water contents of 5%.

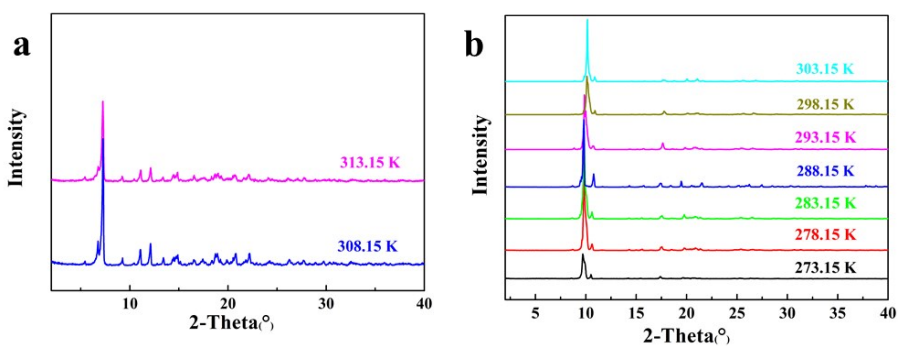


Figure S10. The PXRD pattern of the residual solids after the solubility in water + methanol mixtures with water contents of 15%.

**Table S1.** The solubility of D-PC·MeOH in water + methanol mixtures with water mass content as 2%, 5% and 15%, respectively.

$T/K$	$w_1^0$	$x_1^0$	$10^3 x_A$	$w_1^0$	$x_1^0$	$10^3 x_A$	$w_1^0$	$x_1^0$	$10^3 x_A$
273.15			0.351			0.960			2.812
278.15			0.355			1.008			2.988
283.15			0.360			1.062			3.151
288.15			0.366			1.113			3.317
293.15	2%	0.0350	0.373	5%	0.0850	1.188	15%	0.2388	3.512
298.15			0.379			1.249			3.712
303.15			0.387			1.339			3.961
308.15			0.395			1.383			4.091
313.15			0.413			1.434			4.357

**Table S2.** The solubility of D-PC·4MeOH·H<sub>2</sub>O in water + methanol mixtures with water mass content as 2%, 5% and 15%, respectively.

$T/K$	$w_1^0$	$x_1^0$	$10^3 x_A$	$w_1^0$	$x_1^0$	$10^3 x_A$	$w_1^0$	$x_1^0$	$10^3 x_A$
273.15			0.117			0.160			0.440
278.15			0.172			0.224			0.611
283.15			0.239			0.322			0.877
288.15			0.352			0.476			1.285
293.15	2%	0.0350	0.536	5%	0.0850	0.694	15%	0.2388	1.773
298.15			0.855			1.014			2.482
303.15			1.222			1.439			3.608
308.15			1.618			2.083			4.824
313.15			2.157			2.981			6.256